CONTRIBUTION FROM THE BAKER LABORATORY OF CHEMISTRY,
CORNELL UNIVERSITY, ITHACA, NEW YORK 14850

Solid-State Studies of Oxygen-Deficient Tantalum Pentoxide[1]

BY DANIEL R. KUDRAK AND M. J. SIENKO

Received October 21, 1966

Although several lower oxides of tantalum—*i.e.*, Ta_4O, Ta_2O, TaO, TaO_2, TaO_x ($2 < x < 2.5$)—have been reported in the literature, only the last, TaO_x, could be reproduced in this investigation. Single crystals of composition $Ta_2O_{4.73}$ were prepared by vacuum fusion of Ta_2O_5 in Ta, using radiofrequency induction heating at about 1900°. Potential-probe conductivity studies disclosed metallic behavior, the resistivity rising almost linearly from 0.63×10^{-2} ohm cm at 4.2°K to 4.3×10^{-2} ohm cm at 295°K. Hall voltage measurements indicated n-type carriers at densities of 4.5×10^{20} cm^{-3}, independent of temperature. The Seebeck coefficient was found to change linearly from -10 $\mu v\ deg^{-1}$ at 90°K to -50 $\mu v\ deg^{-1}$ at 300°K. Magnetic susceptibility, measured by the Curie method, was small and negative. Observed properties are consistent with a d-type conduction-band model in which donor centers are so concentrated that degenerate electron gas behavior results. Density data on single crystals suggest that the oxygen defect actually arises from tantalum interstitials. The thermal dependence of carrier mobility is quantitatively consistent with optical mode lattice scattering.

Introduction

Transition metal oxides such as WO_3, V_2O_5, and TiO_2 can be converted from the insulating state to the conducting state by insertion of alkali metal into the oxide matrix. The alkali atom, as an interstitial dopant, can transfer its valence electron to host structure delocalized states, originating either from direct overlap of the transition metal d t_{2g} orbitals[2] or from indirect overlap of d orbitals through intervening oxygen $p\pi$ interactions.[3] At low doping levels—*e.g.*, $x < 0.25$ in the tungsten bronzes M_xWO_3—behavior is semiconductive;[4] at high doping levels—*e.g.*, $x > 0.25$ in M_xWO_3—behavior is metallic.[5] Mott has shown[6] that in general the activation energy for electron transfer should vanish when the mean distance between donor centers is about 4.5 times their radius. In the M_xWO_3 system, using an expanded hydrogenic model with weighted optic and static dielectric constants, this corresponds to $x \approx 0.25$. Another way of introducing donor centers is by removal of oxygen, each missing oxygen atom being equivalent to two added alkali atoms. The equivalence of oxygen defect to alkali addition has been demonstrated in the WO_3 system by the fact that the magnetic behavior as a function of x is the same in WO_{3-x} as in M_xWO_3.[7] Furthermore, as predicted by the Mott theory, again assuming close-packed hydrogenic donors in an effective dielectric medium, there seems to be a crossover from semiconductive to metallic behavior when $^1/_{30}$ of the oxygen atoms have been removed from the WO_3 structure.[8] The same onset of metallic behavior is anticipated in the Ta_2O_5 system.

The purpose of this investigation was to examine the effect of removal of oxygen from Ta_2O_5 and, in particular, to examine by solid-state measurements the carrier characteristics in the resulting materials. Morin's d-orbital overlap criterion suggests that 5d-banded materials should show higher carrier mobility than 4d or 3d. As part of a general study of defect transition metal oxides, it was desirable to have solid-state data for Ta_2O_5 to compare with those already obtained for V_2O_5 and WO_3. The investigation consists of two parts: (1) attempts to prepare lower oxides of tantalum and (2) studies of conductivity, Hall voltage, thermoelectric power, and magnetic susceptibility of the one lower oxide that could be synthesized.

Experimental Procedures and Results

Attempts to Prepare Lower Oxides.—Thermogravimetric monitoring with an Aminco thermobalance of tantalum heated in static air atmosphere showed no oxidation until 600°, at which point weight increased smoothly to a value consistent with Ta_2O_5; there was no sign of plateaus or changes of slope corresponding to formation of lower oxides either on raising the temperature from 600 to 900° or on holding it constant at 610°. Heating of tantalum up to 1250° in carbon monoxide, both static and flowing, produced Ta_2O_5 and TaC, not TaO as reported elsewhere.[9] Attempts to reduce Ta_2O_5 to lower oxides in open-boat reactions were unsuccessful. With Mg in H_2 or Ar atmosphere at 600–650°, the product as monitored by X-ray analysis was Ta metal. With CO at 1200–1450° and H_2 at 1200–1600°, no reduction of Ta_2O_5 was observed. Ta_2O_5 heated with Ta up to 1600° under vacuum or in hydrogen produced only a mixture of Ta_2O_5 and Ta. With carbon, under vacuum or in hyrogen, up to 1600°, Ta_2O_5 formed either carbides or oxycarbides. Sealed-capsule reactions in Vycor or platinum at 950° were equally unsuccessful. Ta plus ZnO gave Ta_2O_5; Ta plus MgO or CaO gave no reaction; Ta plus MnO, V_2O_3, or TiO_2 gave mixed oxides that could not be identified. Ta_2O_5 plus Zn gave no reaction; Ta_2O_5 plus Mn or B gave mixed oxides. Only the reaction between Ta_2O_5 and Ta, at 1450–1500° in platinum for 2 days, produced an oxygen-deficient form of

(1) This research was sponsored by the Air Force Office of Scientific Research, Office of Aerospace Research, United States Air Force, under AFOSR Grant No. 796-65, and was supported in part by the Advanced Research Projects Agency through the Materials Science Center at Cornell University. This report is based on the Ph.D. thesis of D. R. Kudrak.

(2) F. J. Morin, *Bell System Tech. J.*, **37**, 1047 (1958); M. J. Sienko, Advances in Chemistry Series, No. 39, American Chemical Society, Washington, D. C., 1963, p 224; "Chemical Society Symposia, Nottingham 1966," Special Publication 22, The Chemical Society, London, 1966; *J. Am. Chem. Soc.*, **81**, 5556 (1959).

(3) J. B. Goodenough, *Bull. Soc. Chim. France*, **4**, 1200 (1965); *J. Appl. Phys.*, **37**, 1415 (1966).

(4) W. McNeill and L. E. Conroy, *J. Chem. Phys.*, **36**, 87 (1962).

(5) M. J. Sienko and T. B. N. Truong, *J. Am. Chem. Soc.*, **83**, 3939 (1961).

(6) N. F. Mott, *Nuovo Cimento Suppl.*, **7**, 312 (1958); *Phil. Mag.*, **6**, 287 (1961).

(7) M. J. Sienko and B. Banerjee, *J. Am. Chem. Soc.*, **83**, 4149 (1961).

(8) J. Berak and M. J. Sienko, to be published.

(9) A. V. Lapitskii, Y. P. Simanov, and E. P. Artamova, *Zh. Neorgan. Khim.*, **2**, 80 (1957); *Russ. J. Inorg. Chem.*, **2**, 122 (1957).

Ta_2O_5. The conclusion reached from the above experiments was that lower oxides of tantalum such as TaO and TaO_2 do not exist as isolable compounds.

Preparation of Oxygen-Deficient Ta_2O_5.—The crystals obtained from sealed-capsule reactions were less than 1 mm in the longest dimension, too small for normal solid-state measurements. Larger crystals were obtained by radiofrequency induction heating under vacuum of Ta plus Ta_2O_5 mixtures, molar ratios varying from 3:1 to 0:1, to above the melting point of Ta_2O_5 in vessels of tantalum, molybdenum, or tungsten. In all cases, a hard, black, crystalline material was formed. Since the samples containing Ta as a reactant showed some unreacted metal in the product, only crystals prepared by heating pentoxide alone were used for the measurements below. The molybdenum and tungsten vessels were commercial crucibles; the tantalum containers were made from Fansteel seamless tantalum tubing which was cut to the appropriate length, squeezed at one end in a vise, then arc welded closed. The tungsten and molybdenum crucibles were pretreated by heating to 1600° at 10^{-5} torr for 15 min. After being filled with Ta_2O_5 powder, the containers were placed upright in a zirconia crucible which was covered with a zirconia lid having a small hole for optical pyrometer sighting. The zirconia crucible was surrounded by an alundum cylinder as a radiation shield. The entire assembly was supported from below on alundum disks by a stainless steel pedestal and was surrounded by a Vycor tube which was vacuum sealed by a stainless steel plate fitted with a quartz sight glass. The remainder of the vacuum system was all stainless steel. After pumpdown to 10^{-6} torr for several hours, induction heating was gradually increased through saturable reactor power control on the input of the radiofrequency generator. Cooling was relatively quick, 5–10 min for manual decrease of radiofrequency power followed by natural cooling under vacuum to room temperature. Containers were cut open with a water-cooled silicon carbide wheel. Two samples, prepared in tantalum containers, were trimmed without regard for crystallographic orientation for the electric and magnetic study described below.

Analysis of Chemical Composition.—Powder X-ray patterns of portions of the above samples, taken with Cu $K\alpha$ radiation, were identical with those of the high-temperature form of Ta_2O_5.[10] The chemical composition of the crystals was determined, after completion of the electric and magnetic studies, by oxidation of the samples in flowing oxygen at 950° for 1 hr. Assuming that the reaction is

$$Ta_2O_{5-x} + (x/2)O_2 \longrightarrow Ta_2O_5$$

x can be determined by measuring the increase in mass due to oxygen pickup. Sample I, weighing 0.05514 g, absorbed 0.00055 g of oxygen and thus corresponded to an initial composition of $Ta_2O_{4.73}$; sample II, weighing 0.12057 g, absorbed 0.00116 g of oxygen, corresponding to $Ta_2O_{4.737}$.

Density of the Samples.—The densities of the crystals were determined by measuring the buoyancy effect on the sample immersed in water. A correction for the suspending copper wire was applied. The measured density of sample I at 22.8° was 8.74 g/cc; the measured density of sample II at 24.1° was also 8.74 g/cc.

Electrical Resistivity Measurements.—A crystal holder was constructed from prepunched circuit board with two current probes and four potential probes mounted and held on the crystal by mechanical pressure. The current contacts were pieces of copper sheet machined so the entire end of the crystal was covered. Potential probes consisted of two thermocouple beads of 0.003-in. copper and constantan wire on one face of the crystal and two 0.003-in. copper wires on the opposite face. Contact resistances were generally of the order of 2 ohms, compared to a crystal resistance of about 0.1 ohm; these were not operative in the null potentiometric method employed. Temperature variation was provided by nichrome or carbon resistance heaters mounted directly on the crystal holder. The entire circuit board assembly was mounted in a glass tube fitted into another evacuable Pyrex tube, the whole constituting a dewar vessel that could be immersed in a commercial dewar filled with liquid nitrogen.

Standard voltage-drop resistivity measurements were made using both ac and dc techniques. One of the ac systems used the Dauphinee–Mooser[11] chopper technique, in which battery current is passed through a mechanical chopper to give a square-wave current that is fed in series through the crystal and a standard resistor while at the same time a capacitor is switched alternately from standard to unknown at the same frequency and phase as the current. The other ac system used a PAR lock-in amplifier. Dc techniques differed in their sources of constant current; these included a Fluke constant-current supply and a single transistor operating in common-base configuration. Voltage drops across the standard resistor and across the sample were measured either by a Leeds and Northrup K-3 potentiometer or a Keithley 150 AR microvoltmeter.

The results of the resistivity measurements are summarized in Figure 1.

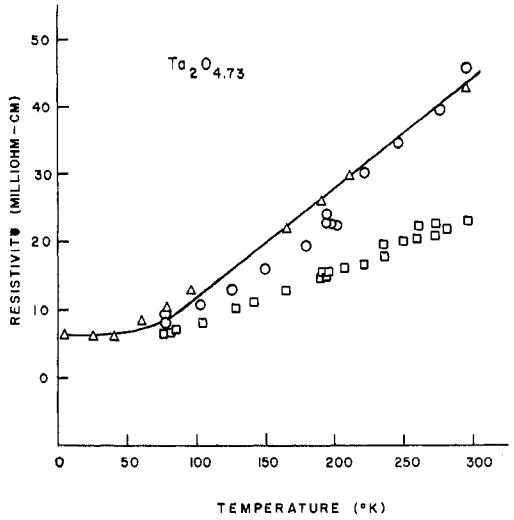

Figure 1.—Resistivity of single crystals of $Ta_2O_{4.73}$ as a function of temperature. Circles and triangles apply to sample I; squares, to sample II. The differing values between samples I and II may be due to differing crystallographic orientation with respect to sample geometry. The solid curve, which by change in choice of constants can be made to fit sample II equally well, is calculated from eq 1.

Thermoelectric Power.—A thermal gradient was produced across the crystal by two small heaters attached to the current contacts. The thermal emf of each thermocouple bead and the emf developed between the copper leads of the two thermocouples were measured with the K-3 potentiometer. The thermoelectric power $\Delta V/\Delta T$ was independent of ΔT, which was generally of the order of 1°. Results are summarized in Figure 2.

Hall Effect.—The Hall effect measurements were obtained using dc current from a 6-v storage cell; the Hall voltage was measured by the Keithley microvoltmeter, the output of which was fed to a Varian G-11A strip-chart recorder. In the absence of the magnetic field, a voltage null was obtained by establishing a virtual equipotential plane with the aid of a misalignment potentiometer. Both current and magnetic field directions were reversed and the difference in voltage with reversal was taken as twice the Hall voltage. Magnetic fields, up to 8000 gauss, were furnished by a water-cooled 6-in. electromagnet.

Hall voltage measurements were made only on sample I, but the close correspondence of other properties between samples

(10) S. Lagergren and A. Magnéli, ASTM Powder Diffraction File Card No. 5-0258.

(11) T. M. Dauphinee and H. Preston-Thomas, *J. Sci. Instr.*, **35**, 21 (1958); see also B. L. Crowder, Ph.D. Thesis, Cornell University, 1963.

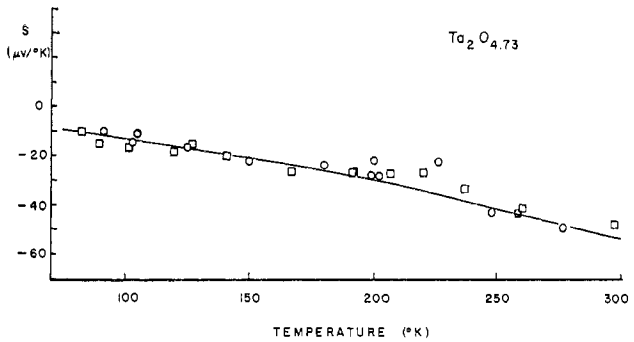

Figure 2.—Thermoelectric power of single crystals of $Ta_2O_{4.73}$ as a function of temperature. Circles refer to sample I; squares, to sample II. The solid curve is calculated from eq 2.

I and II suggests an identity of all characteristics. The data analysis that follows holds strictly for sample I. Sample I was 0.365 cm in length, 0.195 cm in width, and 0.135 cm in thickness. At 273°K with 0.200 amp in a field of 6100 gauss, the Hall effect amounted to 1.2×10^{-6} v, corresponding to a Hall coefficient R of -1.4×10^{-2} cc/coulomb. (A shape factor S equal to 0.92 was used in computing from $R = 10^8 vt/IHS$.) At 77°K, the same crystal had a Hall coefficient of -0.90×10^{-2} cc/coulomb. Using $R = A/ne$ (A, the scattering factor, was assumed to be unity), the charge carrier density n is 4.5×10^{20} electrons/cc at 273°K and 6.9×10^{20} at 77°K. The difference between the two values is not considered to be significant, first, because the signal-to-noise ratio was poorer at the low temperature, where there was difficulty in maintaining constant current through the crystal contacts, and, second, because no appreciable carrier density variation is expected for a system well below its degeneracy temperature. With a carrier density of about 5×10^{20} cc^{-1}, the degeneracy temperature, $T = (3n/\pi)^{2/3}(h^2/8km)$, is about 2500°K. Because the 273°K measurement was the more reliable, we consider in the Discussion that the carrier density is independent of temperature and equal to 4.5×10^{20} cc^{-1}.

Magnetic Susceptibility.—Measurement was by the Curie method. The sample, in the shape of a rectangular parallelipiped, was suspended by a thread in the gap of an electromagnet near the top of the tapered pole pieces. The change in weight on application of the field was determined with an Ainsworth semimicro analytical balance. Calibration was by a sodium chloride crystal of approximately the same size. At maximum magnetic field (about 6000 gauss), the observed weight change for sample I (volume 9.55×10^{-3} cc) was -50 μg and for NaCl (volume 7.15×10^{-3} cc) it was -125 μg. Since the measurements were performed in air, a correction for the volume susceptibility of air was applied. Using -1.1×10^{-6} and $+0.029 \times 10^{-6}$ for the volume susceptibilities of NaCl and air, respectively, one obtains -0.31×10^{-6} for the volume susceptibility of $Ta_2O_{4.7}$. This corresponds to a gram susceptibility of -0.035×10^{-6}. Because the forces measured were so very small, the estimated precision on this value is ±50%.

Discussion

The general behavior of the $Ta_2O_{4.73}$ samples is that of a highly degenerate impurity metal, dominated at higher temperatures by optical mode lattice scattering and at lower temperatures by impurity scattering. This is in contrast to the semiconduction behavior reported by Kofstad[12] and Sokalski and Czarny[13] for powder specimens of tantalum pentoxide sintered in air and measured at various oxygen pressures. Kofstad, in particular, found p-type semiconducting behavior for a sample measured at high oxygen pressures (*i.e.*, about 1 atm) and n-type behavior at low oxygen pressures (*i.e.*, down to 10^{-18} atm). He interpreted his results in terms of oxygen interstitials for the p-type material and oxygen vacancies for the n-type. Such a model could be carried over to account for our metallic findings, since sufficiently high n-type doping with oxygen vacancies would give degenerate metal behavior. However, it may be that the behavior remarked for powders, particularly the p-type conduction, is due to grain contact effects not directly relatable to bulk resistivity characteristics.

The notable features of the resistivity data of Figure 1 are constant resistivity at low temperatures and the nonlinear increase at higher temperatures. The observed resistivity ρ can therefore be considered the sum of ρ_r, a residual part, and ρ_T, a temperature-dependent part. ρ_r is usually ascribed to electron scattering by impurities, which in this case may be either neutral or ionized, since scattering by each of these is independent of temperature. ρ_T can be shown to fit the theory of optical mode phonon scattering in polar semiconductors. The theory, developed by Howarth and Sondheimer[14] and successfully applied by Crowder and Sienko to the tungsten bronzes,[15] predicts the conductivity σ_T to follow the dependence

$$\sigma_T = cT \sinh^2 (\theta/2T) \qquad (1)$$

where c is a constant depending on θ and the Fermi energy E_F, and θ is the Debye temperature of the lattice. θ is not known but may be estimated by noting that for most metals, the transition from T^5 to T^1 dependence in the ρ_T *vs.* T curve occurs at a temperature of approximately $\theta/7$. For sample I, a similar type of transition occurs at about 50°K, leading to a θ of about 350°K. Once θ is known, c can be evaluated from a measured value of ρ_T. Taking ρ_r to be 0.63×10^{-2} ohm cm, c is 0.232 (ohm cm deg)$^{-1}$. The solid curve shown in Figure 1 is calculated using these parameters.

The Hall mobility μ_H of the charge carriers can be determined from $\mu_H = |R|\sigma = |R|/\rho$, where $|R|$ is the magnitude of the Hall coefficient, provided that only one type of charge carrier is present. Since the total resistivity ρ is assumed to be the sum of a residual part and a temperature-dependent part, mobilities associated with the two mechanisms can be assumed to add reciprocally

$$\mu_H^{-1} = \mu_r^{-1} + \mu_T^{-1}$$

where μ_r is the temperature-independent mobility due to scattering by impurities and μ_T is the "thermal" mobility associated with the temperature-dependent lattice scattering. Assuming that the number density of carriers is constant with temperature (as discussed above under Hall effect), the thermal dependence of the "thermal" mobility can be deduced from the thermal dependence of the conductivity. Table I gives a comparison of the experimental mobilities with those calculated from the Howarth–Sondheimer dependence,

(12) P. Kofstad, *J. Electrochem. Soc.*, **109**, 776 (1962).
(13) Z. Sokalski and Z. Czarny, *Roczniki Chem.*, **39**, 299 (1965).
(14) D. J. Howarth and E. H. Sondheimer, *Proc. Roy. Soc.* (London), **A219**, 53 (1953).
(15) B. L. Crowder and M. J. Sienko, *J. Chem. Phys.*, **38**, 1576 (1963).

$aT \sinh^2 (\theta/2T)$, and with those calculated assuming a $bT^{-3/2}$ dependence, characteristic of acoustic mode scattering. The constants, a and b, evaluated from fitting the experimental point at 300°K, have values of 3.24×10^{-3} cm²/v sec deg and 1.92×10^{3} cm² deg$^{3/2}$/v sec, respectively. μ_r is 2.2 cm²/v sec. Although both $aT \sinh^2 (\theta/2T)$ and $bT^{-3/2}$ satisfactorily reproduce the data, the latter appears ruled out on the basis that the constant b is much smaller than is usually associated with acoustic mode scattering.

TABLE I

CARRIER MOBILITY DATA FOR $Ta_2O_{4.7}$

Temp, °K	$10^2\rho_T$, ohm cm	Exptl μ_T, cm²/v sec	Calcd $aT \sinh^2 (\theta/2T)$	Calcd $bT^{-3/2}$
50	0.09	16	44	5.4
100	0.65	2.2	2.5	1.9
150	1.32	1.1	1.0	1.0
200	2.07	0.68	0.64	0.68
250	2.97	0.47	0.47	0.49
300	3.77	0.37	...	...

Figure 2 shows an almost linear change of thermoelectric power with temperature, as predicted for highly degenerate polar semiconductors by the Howarth–Sondheimer theory. The solid curve of Figure 2 is calculated by eq 2 where S is the thermoelectric

$$S = \frac{\pi^2 k^2 T}{3eE_F} \frac{4\pi^2 - 2z^2 + 3z^2 \ln 4(E_F/k\theta)}{2\pi^2 - z^2 + 3z^2 \ln 4(E_F/k\theta)} \qquad (2)$$

power, E_F is the Fermi energy, and z is the ratio θ/T. The Fermi energy of a degenerate system of electrons can be calculated from

$$E_F = (h^2/8m^*)(3n/\pi)^{2/3} = 3.61 \times 10^{-15}(m/m^*)n^{2/3}$$

where m^* is the effective mass of the electron. Since the weak dependence on E_F of the bracketed term in eq 2 can be neglected, E_F and hence m^* can be deduced from experimental values of S. With $n = 4.5 \times 10^{20}$ cc^{-1}, E_F is 0.21 ev and m/m^* is 1.0.

The source of conduction electrons in $Ta_2O_{4.73}$ can be attributed to deviation from Ta_2O_5 stoichiometry, brought about either by the absence of oxygen atoms from normal lattice sites or by the presence of extra tantalum atoms in interstitial positions. The density data give a strong argument for believing in tantalum interstitials. Reisman, *et al.*,[16] determined pycnometrically that the density of the high-temperature form of Ta_2O_5 is 8.37 ± 0.01 g/cc. If the lattice parameters do not change (X-ray patterns are identical), the density of $Ta_2O_{4.73}$ (or $Ta_{2.11}O_5$) can be calculated by adding to 8.37 g/cc the contribution of 0.11 g-atom of Ta/mole of Ta_2O_5—*i.e.*, 0.38 g/cc. The total calculated density, 8.75 g/cc, compares satisfactorily with the observed value of 8.74 g/cc. A more detailed understanding of the oxygen vacancy *vs.* tantalum interstitial problem is hindered because the crystal structure of high-temperature Ta_2O_5 is largely unknown. The unit cell for high-temperature Ta_2O_5 is reported[17] to be tetragonal with dimensions 3.80 × 3.80 × 35.60 A. The precision is not adequate to exclude completely the possibility of oxygen vacancies.

If the conduction electrons in $Ta_{2.11}O_5$ indeed originate from tantalum interstitials, there is still an unresolved factor between the observed electron density of 4.5×10^{20} cc^{-1} and that predicted from 1.25×10^{21} excess Ta atoms/cc. Several explanations suggest themselves: (1) there may be two kinds of Ta interstitials, one being easily ionized and the other giving strongly bound lower levels; (2) there may be a significant difference between the Hall mobility and the actual drift mobility of the carriers; (3) there may be compensation by acceptor centers which trap some of the carriers. The fact that Laue back-reflection X-ray photographs of both samples I and II show them to be highly strained and rather imperfect crystals suggests that they are rich in defects. These defects may act as trapping centers and, in fact, may account for the relatively large residual resistivity observed. Defects with trapped electrons would scatter as ionized impurities, leading to a residual mobility given by

$$\mu_r = \frac{3h^3\kappa^2 n}{16\pi^2 e^3 m^2 f(x) N_i}$$

κ is the effective dielectric constant, N_i is the concentration of ionized centers, and $f(x) = \ln(1 + x) - (x/(1 + x))$ with $x = {}^1/_2(h/e)^2(\kappa/m)(3n/8\pi)^{1/3}$. For κ, we can use the weighted mean of the static dielectric constant ϵ and the optical dielectric constant ϵ_0 as suggested by Crowder and Sienko.[15] With $\epsilon_0 = 5.2$ and $\epsilon \approx 40$, κ is about 13. If each interstitial Ta makes available one electron, there would be a total of 1.25×10^{21} cc^{-1}. If only 4.5×10^{20} cc^{-1} were free, the remaining 8×10^{20} cc^{-1} would have to be trapped out to give negative defects. N_i, the total concentration of ionized centers, would then be the sum of the Ta^+ concentration (1.25×10^{21}) and the defect concentration (8×10^{20}). The expected residual mobility would be about 9 cm²/v sec, compared to 2.2 cm²/v sec actually observed.

The measured value of the volume susceptibility of $Ta_2O_{4.73}$, $\kappa = -0.31 \times 10^{-6}$, is close to the value of the volume susceptibility of Ta_2O_5, -0.53×10^{-6}, previously measured in this laboratory. The difference between the two values is close to the value $+0.11 \times 10^{-6}$ calculated for a collection of 4.5×10^{20} electrons cc^{-1} by the Pauli paramagnetism $\kappa = n\mu_B^2/kT_F$, where μ_B is the Bohr magneton and T_F is the Fermi degeneracy temperature.

The most striking property of the above material is the metallic behavior and its persistence to very low temperatures. There are three possible interpretations of this behavior: (I) the material contains donor centers that lie in or above a d-type conduction band of the host material; (II) the donor centers lie just below the conduction band but are so concentrated that the Fermi level has moved into the conduction band;

(16) A. Reisman, F. Holtzberg, M. Berkenblit, and M. Berry, *J. Am. Chem. Soc.*, **78**, 4514 (1956).

(17) A. I. Zaslavskii, R. A. Zvinchuk, and A. G. Tutov, *Dokl. Akad. Nauk SSSR*, **104**, 409 (1955).

(III) the donor centers are deep in the forbidden gap but are so concentrated that wave functions overlap and "impurity band" conduction results. In the case of alkali-doped transition metal oxides, models I and III appear to be excluded—model I, because it predicts metallic behavior at all concentrations of donor centers (whereas low concentrations of M or of oxygen defect in WO_3 result in semiconductivity), and model III, because it predicts that the conduction band wave functions should have substantial donor atomic orbital character (whereas nmr studies suggest such contributions are negligible). Model II thus appears the most suitable; it can be visualized as resulting from a cooperative ionization of all of the donor centers because of mutual screening by all of the delocalized electrons against recapture of electrons by the ionized donor centers.

However, it may not be so easy to distinguish models I, II, and III as the above implies. In Li_xWO_3, for example, it has been suggested[5] that the donor center is not simply the Li atom in the host WO_3 matrix but rather the cage of tungsten atoms around the Li^+ to which the electron has been transferred. Such a transfer complicates matters enormously because the impurity level (Li^0) is definitely above the conduction band, the actual donor center (Li^+-centered tungsten cage with associated electron) is below the band, and, most important of all, the orbitals contributing to the conduction band (nonperturbed W atoms) are very similar to the orbitals describing the localized electron (perturbed W atoms). With increasing impurity concentration, the onset of metallic behavior can be described equally well as resulting from overlap of the actual donor centers or from cooperative ionization of the donor centers into a host conduction band.

In $Ta_{2+x}O_5$, the tantalum interstitials may themselves be the donor centers, in which case model I would require them to lie above the Ta_2O_5 conduction band whereas model II would place them just below the conduction band but at such high concentration that degenerate electron behavior results. Model III would appear to be unsuitable for this material since the spacing between Ta interstitials is greater than between Ta interstitials and Ta normal sites. Models I and II could be distinguished by studying the behavior at low concentration of Ta interstitials. (We tried to do this but found that the material could not be synthesized with less than a large concentration of interstitials.) At low concentration of interstitials, model I would predict zero activation energy for electron transport, and model II would predict finite activation energy provided the concentration of interstitials was low enough. An alternate picture is that the Ta interstitials are not the donor centers but have transferred their electrons to other structural features (*e.g.*, dislocations) which then act as donor centers. In such case, metallic behavior could also result if the donor density were high enough to produce degenerate behavior.

CONTRIBUTION NO. 66-34 FROM THE COLLEGE OF EARTH AND MINERAL SCIENCES, THE PENNSYLVANIA STATE UNIVERSITY, UNIVERSITY PARK, PENNSYLVANIA 16802

Phase Relationships in the System SrO–P_2O_5 and the Influence of Water Vapor on the Formation of $Sr_4P_2O_9$

BY ERIC R. KREIDLER AND F. A. HUMMEL

Received October 21, 1966

Phase relationships in the system SrO–P_2O_5 were determined by quenching, strip furnace, vacuum heat treatment, and high-temperature X-ray diffraction methods. The results of experiments done in air at temperatures below 1400° on compositions near the SrO end of the system can be interpreted only by considering water vapor as a component of the system. The data were used to construct phase diagrams for the system SrO–P_2O_5 and a portion of the system SrO–P_2O_5–H_2O. The melting behavior and polymorphism of the six binary compounds is discussed in detail. The SrO–P_2O_5 system is compared with the previously reported CaO–P_2O_5 system. Limited data for the CaO–P_2O_5 system indicate errors in the reported diagrams, and a new diagram for the CaO–P_2O_5 system is proposed, but it is emphasized that a careful reinvestigation of this system is needed.

Introduction and Literature Survey

The SrO–P_2O_5 system is of technological importance because two of the compounds in the system, $Sr_2P_2O_7$ and $Sr_3(PO_4)_2$, serve as host structures for efficient tin-activated (Sn^{2+}) phosphors.

Although no phase diagram has been published for the SrO–P_2O_5 system, Ropp, Aia, Hoffman, Veleker, and Mooney[1] have published very reliable X-ray diffraction patterns for most of the anhydrous compounds and their polymorphs. The phases reported were: γ-, β-, and α-strontium metaphosphate, $Sr(PO_3)_2$; β- and α-strontium pyrophosphate, $Sr_2P_2O_7$; strontium orthophosphate, $Sr_3(PO_4)_2$; and strontium hydroxylapatite, $Sr_{10}(PO_4)_6(OH)_2$. The phase transitions were studied by differential thermal analysis and thermogravimetric analysis. The following transition points were found

(1) R. C. Ropp, M. A. Aia, C. W. W. Hoffman, T. J. Veleker, and R. W. Mooney, *Anal. Chem.*, **31**, 1163 (1959).